Journal of Chromatography, 387 (1987) 21–40
Elsevier Science Publishers B.V., Amsterdam — Printed in The Netherlands

CHROM. 19 055

PREDICTING BANDWIDTH IN THE HIGH-PERFORMANCE LIQUID CHROMATOGRAPHIC SEPARATION OF LARGE BIOMOLECULES

II*. A GENERAL MODEL FOR THE FOUR COMMON HIGH-PERFORMANCE LIQUID CHROMATOGRAPHY METHODS

M. A. STADALIUS
Agricultural Chemicals Dept., E. I. Du Pont de Nemours & Co., Wilmington, DE 19898 (U.S.A.)
B. F. D. GHRIST
Biomedical Products Dept., E. I. Du Pont de Nemours & Co., Wilmington, DE 19898 (U.S.A.)
and
L. R. SNYDER*
LC Resources, Inc., 26 Silverwood Court, Orinda, CA 94563 (U.S.A.)
(First received August 21st, 1986; revised manuscript received September 4th, 1986)

SUMMARY

A general model for describing gradient elution separations of peptides and proteins by reversed-phase high-performance liquid chromatography (HPLC) has been presented previously. This model has now been modified so that it can be applied to any of the four HPLC methods used for separating biological macromolecules: reversed-phase, ion-exchange, hydrophobic-interaction and size-exclusion chromatography, carried out in either an isocratic or gradient elution mode. The role of sample molecule structure and the particular column used has been further studied, so that previous empirical parameters for different column/sample choices can now be estimated from three physical properties of the sample and the column: (a) sample molecular weight, (b) native *vs.* denatured sample, (c) column packing pore diameter. This eliminates much of the empiricism of our preceding model, and minimizes the number of experimental runs now required in order to apply the model in practice.

The final model has been tested for (a) several hundred runs involving peptides and proteins in the molecular weight range 600–162 000, (b) all four of these HPLC methods, (c) in both isocratic and gradient elution modes, and (d) using data from several different laboratories (including our own). The model is able to predict bandwidth in HPLC separations of proteins and peptides with an accuracy of ±17% (1 standard deviation), for the case of "well-behaved" separations. Separations that are not "well-behaved" will give wider bands than predicted by the model.

* For Part I see ref. 15.

0021-9673/87/$03.50

INTRODUCTION

The chromatographic separation of large biomolecules is usually a complex process, one that we seldom understand in detail for any given sample. As a result most such separations are developed more or less empirically and non-optimally. This problem becomes more serious as the mass of the sample (and size of the column) increases, and it is likely that an altogether different approach will be required for preparative separations on a process scale.

What is needed for both large- and small-scale applications is a quantitative model of separation, one based on the fundamental processes that control these separations. Since these basic processes are similar for different forms of liquid chromatography (LC), a single model should be capable of describing all such separations: reversed-phase chromatography, ion-exchange chromatography (IEC), hydrophobic-interaction chromatography (HIC) and size-exclusion chromatography (SEC). The model should rely on a minimum of empirical assumptions or fitting-parameters, and its use for predicting separation should not require information other than that available from the usual experimental runs with the sample of interest. The application of the model should reduce the actual number of runs required in developing a final high-performance liquid chromatography (HPLC) procedure, and the final procedure should be more nearly optimal.

The present study continues our attempts at developing such a model, based on (a) initial clarification of the HPLC separation of small molecules by isocratic or gradient elution[1–6], (b) the extension of this picture to large synthetic polymers[7–10], and (c) the application of these concepts to the gradient separation of peptides and proteins by reversed-phase chromatography[10–13] and IEC[14]. In the present and preceding paper[15] we provide additional experimental data to (a) further confirm this model and (b) better define the dependence of these separations on the molecular structure of the sample and the physical properties of the column packing. This information has led to a significant modification of our original model, with an expansion of its applicability and a reduction in the number of empirical parameters that must be measured. Finally, in this paper we will summarize all the bandwidth data so far used to develop and test the model, and we will examine its overall accuracy.

THEORY

The model presented earlier[10–14] and further developed here can be summarized as follows:

(1) The HPLC separation of large molecules is governed by the same principles that apply for the isocratic or gradient separation of small molecules.

(2) Retention and bandwidth can be predicted for any compound as a function of experimental conditions, given certain initial data (values of K, S or m)* that are derivable from two initial runs (gradients with only t_G varied).

(3) When experimental bandwidths differ from those predicted by the model, the experimental values will be larger, and this implies that the sample (protein) is

* For list of symbols see Part I (ref. 15).

not "well behaved"; we need then to explore ways to minimize these non-ideal effects and thereby improve the separation.

Previous papers from this and other laboratories[13–23] have illustrated the various ways in which our model can be applied to improving and understanding practical protein separations by HPLC.

The final form of our model for general application to any HPLC procedure is detailed in Appendix I. In this paper we will discuss various additions and modifications relative to the model described in refs. 11, 13 and 14. We will also further examine some of the empirical relationships which facilitate various applications of this model.

Knox equation

Our calculation of bandwidths uses the Knox equation[24]

$$h = Av^{1/3} + B/v + Cv \tag{1}$$

which was discussed in ref. 15. We have previously approximated the value of v from

$$v = ud_p/D_m \tag{2}$$

with the average mobile phase velocity u (cm/s) given by

$$u = LF/V_m \tag{3}$$

Here, d_p is the column packing particle diameter, D_m is the solute diffusion coefficient, L is the column length, F is the mobile phase flow-rate, and V_m is the dead-volume of the column.

Fundamental equations for C[25] (which we will discuss) are related not to u, but to the superficial velocity u':

$$u' = u/x, \tag{4}$$

where x is the fraction of mobile phase within the column and outside of the pores. In this paper we will therefore use the superficial reduced velocity

$$v' = u'd_p/D_m \tag{5}$$

in place of v (see also examples of Appendix I).

V_m can be approximated by

$$V_m = (0.4/x)\,(\pi/4)d_c^2L \tag{6}$$

Eqn. 6 assumes that the fraction of the column space between particles of column packing is equal to 0.4; x is the fraction of mobile phase within the column that is contained outside of the pores, d_c is column diameter and L is column length (see discussion of Stout *et al.*[5]).

Knox parameter A. The parameter A of eqn. 1 can be obtained as originally described in ref. 5. A is a constant for a given column and any solute or set of

experimental conditions; it can be measured experimentally by fitting eqn. 1 to experimental data for bandwidths as a function of flow-rate; the best value of A gives the closest agreement between calculated and experimental bandwidth values. Values of A for a well-packed column fall within narrow limits: $0.5 \leqslant A \leqslant 1.0$. We have not changed the way in which A is determined (model of Appendix I).

Knox parameter B. The parameter B of eqn. 1 was previously given as

$$B = a' + b'k' \tag{7}$$

The quantity a' was found equal to 1.1 (within experimental error, ref. 5) for a number of HPLC systems involving small molecules; our previous model assumed $a' = 1.1$ for peptides and proteins as well. The parameter b' measures the relative diffusion of sample molecules in the stationary *vs.* mobile phases; B is seen to increase with increase in the sample capacity factor k' (for gradient elution, k' is replaced by the effective capacity factor $\bar{k}$).

Further analysis of the parameter B yields an exact expression[5]

$$B = 1.28[x + (1-x)(D_p/D_m) + k'(D_s/D_m)] \tag{8}$$

which is seen to have the same form as eqn. 7. Here D_p is the solute diffusion coefficient in the mobile phase contained within the packing pores; D_s is the corresponding quantity for diffusion of solute molecules in the stationary phase (D_m is the diffusion coefficient in the bulk mobile phase). The important quantity (D_p/D_m) was discussed in detail in the preceding paper[15]:

$$\rho^* = (D_p/D_m) \tag{9}$$

We can express (D_s/D_m) as $[(D_s/D_p)/(D_p/D_m)]$, so that eqn. 8 becomes

$$B = 1.28\,[x + \rho^*(1-x)] + 1.28\,[\rho^*(D_s/D_p)\,k'] \tag{10}$$

The quantity (D_s/D_p) is another fundamental parameter; it represents the diffusion-rate of solute molecules that are retained in the stationary phase *vs.* diffusion in the adjacent mobile phase within the pore. Comparison of eqn. 7 with eqn. 10 then gives

$$a' = 1.28\,[x + \rho^*(1-x)] \tag{11}$$

and

$$b' = 1.28\,\rho^*(D_s/D_p) \tag{12}$$

Eqn. 11 shows that the assumption $a' = 1.1$ is not always reliable. Thus for the combination of large molecules and small pores, ρ^* can be quite small. Since x further varies from 0.4 to 0.8 for different columns, a' can range from $0.5 \leqslant a' \leqslant 1.3$. This in turn can have a large effect on predictions of bandwidth by the model, because (see below) the parameter C is a function of B. In the revised model of Appendix I, a' is now calculated from eqn. 11, using values of ρ^* estimated as described later. Similarly the value of b' used in the revised model is now calculated from eqn. 12.

Values of (D_s/D_p) vary with sample molecular weight and the LC method used (*e.g.*, reversed-phase *vs.* ion-exchange), as will be described later.

Knox parameter C. This quantity was given as (eqn. 19 of ref. 11)

$$C = [(1-x+k')/(1+k')]^2(D_m/\tilde{D}_p)/30(1-x)\gamma\rho \tag{13}$$

Here γ is a tortuousity factor (equal to 0.64) and $\tilde{D}_p$ is the effective (average) diffusion coefficient inside the particle, equal to the combined diffusion coefficient in the mobile and stationary phases within the pore. Eqn. 13 is actually in error by omission of a term (x) in the numerator of the right-hand-side. This error originally arose as a result of confusion between the use of average velocity u *vs.* superficial velocity u'. The effects of this error were obscured in previous correlations of the model with experimental data, because (a) x did not vary widely in these studies, and (b) resulting errors were partly absorbed into the model's fitting-parameters (b', ρ). The correct form of eqn. 13 is:

$$C = [(1-x+k')/(1+k')]^2x(D_m/\tilde{D}_p)/30(1-x)\gamma\rho \tag{13a}$$

The quantity ρ was originally[5] a different kind of restricted-diffusion parameter, one arising from the "trapping" of small molecules within constricted regions inside the pores of the column packing. Subsequently ρ was interpreted more broadly[12,13], as also reflecting restricted diffusion of large molecules within small pores. However eqn. 13 shows that the term $(\tilde{D}_m/D_p)$ already recognizes the latter effect. Since we now believe that restricted diffusion of the first kind (as measured by ρ) is unimportant for larger molecules, we can assume $\rho = 1$ for the case of large solute molecules.

Values of ρ previously reported[12–14] for peptide/protein separations also reflect contributions from $(\tilde{D}_p/D_m)$, where[5,11]

$$\tilde{D}_p/D_m = [(B/2\gamma) - x]/(1-x) \tag{14}$$

We now know that our calculation of B from eqn. 7 (with $a' = 1.1$) can be in error, and this error was partly compensated by derived values of $\rho \neq 1$. Our revised model assumes that $\rho = 1$, and (D_p/D_m) is now calculated from eqns. 10 and 14. This means that the previous fitting parameters a', b' and ρ of the old model[12–14] are replaced by ρ^* and (D_s/D_m) in the new model. Because these latter parameters (ρ^* and D_s/D_m) are fundamentally based, and refer to specific physical phenomena, they can be related to the properties of the solute/pore system. This means that values of ρ^* and D_s/D_m from different studies should correlate with sample/column physical properties; the resulting correlations should then allow prediction of ρ^* and D_s/D_m for any HPLC system. We will see that this is the case.

Solute diffusion coefficients

It is necessary to estimate the solute diffusion coefficient D_m for any set of experimental conditions, including the choice of sample and column. We will use the empirical equation given in the preceding paper (eqn. 16b)[15]. Since reliable estimates of D_m as a function of experimental conditions are essential to the present model, we should note two additional complications: the pressure dependency of D_m, and the

dependence of D_m on the conformation of the protein molecule (native or denatured).

Dependence of D_m on pressure. As the average pressure within the column increases, D_m values decrease by roughly 0.1% per bar, and this affects the apparent values of A and C in eqn. 1[26]. It has been brought to our attention[27] that this might affect the accuracy of our present model. Biochemical separations such as those treated by our model are typically carried out at lower flow-rates with pressures under 1000 p.s.i. (*e.g.* refs. 13 and 14), however, so that variation in D_m as a result of change in pressure would be expected to be less than 5%. This could result in larger errors in the estimation of values of A and C[26], but this will have relatively little impact on bandwidth values predicted by our model. Thus best-fit values of A (from the application of our model to various systems) have so far fallen in the range $0.6 \leqslant A \leqslant 1.0$, and predicted bandwidth values show little change as A is varied by as much as ± 0.2 units. Values of C might be in error by as much as 10–20%, but these errors tend to cancel when the model is used finally to predict bandwidths for other HPLC systems. See the further discussion of Appendix II.

D_m as a function of protein conformation. This was discussed in detail in the preceding paper[15]. We have measured the apparent increase in protein molecular size upon denaturation (using SEC), and related this to an apparent molecular weight M_d for the denatured compound. This in turn allows prediction of D_m for the denatured protein, using M_d in place of M:

$$M_d = 0.135\, M^{1.4} \tag{15}$$

Band widths in the other HPLC methods

Ion-exchange chromatography. A preliminary account has been reported[15] for the extension of our model to IEC. The basic problem in adapting our linear-solvent-strength (LSS) model (see ref. 1) of gradient elution to ion-exchange separations is that linear salt concentration gradients (normally used in ion exchange) do not yield the required relationship of retention with time during the run:

$$\log k_i = \log k_0 - b(t/t_0) \tag{16}$$

Here k_i refers to k' at the column inlet, b is a constant for a given run, t is the time after the start of the gradient, and t_0 is the column dead-time (k_i at time zero = k_0). This problem has been discussed in detail[4]; it is of minor significance for proteins with an effective charge m^* equal to 3 or more. That is, the model for ion exchange becomes quite similar to that for reversed-phase HPLC in this case ($m \geqslant 3$), and errors resulting from the non-LSS nature of linear-gradient ion-exchange separations are then minor. Our present treatment as presented in Appendix I is more general (see also refs. 4 and 14), and is relatively free from error for any value of m,

Hydrophobic-interaction chromatography. HIC routinely uses gradient elution,

---

* For a monovalent salt used in the ion-exchange gradient (*e.g.*, chloride), the protein k' value is related to salt concentration c as

$$k' = Kc^{-m} \tag{17}$$

where K is the ion-exchange distribution constant for a given protein and ion-exchange system.

with the salt concentration in an aqueous mobile phase decreasing linearly with time (*e.g.*, from 4 to 0.5 *M* ammonium sulfate in 60 min). Values of k' (or $\bar{k}$) have been shown to vary with salt concentration c (*e.g.* refs. 20 and 28) as

$$\log k' = \log k_0 + S\varphi \tag{18}$$

where φ represents (in this case) the volume fraction of low-salt buffer added to the high-salt buffer. The value of S then equals $\log(k_0/k_z)$, where k_z is the value of k' using the second solvent (solvent B, low salt concentration) as mobile phase. Using linear salt gradients, the resulting HIC separations are of the LSS type, and the various equations for reversed-phase HPLC can be used directly.

Melander *et al.*[28] have treated the theory of HIC retention in gradient elution, and have shown qualitatively that experimental data follow their theory. Whereas these authors[28] consider the specific case of early or late elution of solute bands, we will assume generally that elution of sample bands occurs under "gradient" conditions (k_0 large and $t_g < [t_G + t_0 + t_D]$); t_g is solute retention time, t_G is the gradient time t_0 is the column dead-time, and t_D is the dwell time of the gradient equipment[2].

The nomenclature of ref. 28 differs from that used here in terms of defining isocratic retention as a function of salt concentration c:

$$\log k' = \log k_0 + \lambda c \tag{19}$$

In terms of our terminology and that used in ref. 20,

$$S = \lambda(c_0 - c_f) \tag{20}$$

or

$$\lambda = [\log(k_0/k_z)]/(c_0 - c_f) \tag{20a}$$

Here c_f is the final concentration of salt in the gradient, and c_0 is the initial concentration.

Our model treats HIC separation in similar fashion as for reversed-phase HPLC. The main differences are:

(1) We (initially) assumed native proteins in HIC and denatured proteins in reversed-phase LC*, based on the usual state of protein molecules following their HPLC separation.

(2) Change in k' with mobile phase composition (parameter S in reversed-phase) can be estimated as a function of solute molecular weight for reversed-phase, but not (as yet) for HIC; however values of S can be determined from two experimental runs (see ref. 4).

Size-exclusion chromatography. The adaptation of our model for this LC method is described in the preceding paper[15].

---

* Peptides and proteins generally denature during separation by reversed-phase HPLC, but in most cases involving molecules smaller than 30 000 Dalton this process is reversible, so that biologically active solutes can be recovered as final product. See further discussion of refs. 29 and 30.

RESULTS

Previous papers[12–15,17] have summarized a large data-base for peptide and protein bandwidths as a function of experimental HPLC conditions, using various LC methods. These bandwidth data were correlated previously with an earlier version of the present model. Here we wish to reexamine this data-base in terms of the latest version of our model, as described in this paper. We will also include some additional data from the literature.

In applying the present model it is necessary to specify whether sample molecules are in the native or denatured state during separation. As a starting point, we will assume that the solute conformation during separation is as follows: for SEC, IEC and HIC, the native molecule; for reversed-phase, the denatured molecule. These assumptions are based on the fact that reversed-phase separations generally result in denaturation of peptide and protein samples (during separation), while the remaining HPLC methods generally yield undenatured fractions. However these generalizations will undoubtedly fail in specific cases (*e.g.* ref. 29). Caution should therefore be exercised when assuming that the protein sample is in either a native or denatured state during HPLC separation.

Solute molecular size and pore diameter: their effect on values of ρ^* and (D_s/D_m)

Restricted-diffusion parameter ρ^*. For the case of cylindrical pores and native globular proteins (spheres), it has been shown that ρ^* is related to the ratio r_{sp} = (solute Stokes diameter)/(pore diameter) as[31]

$$\rho^* = 1 - 2.10r_{sp} + 2.09r_{sp}^3 - 0.95\, r_{sp}^5 \qquad (21)$$

Various workers[32,33] have used eqn. 21 as a basis for estimating the restriction of diffusion within the pores of HPLC column packings. Walters[32] showed that eqn. 21 gives a good account of column plate numbers in SEC, but his use of an empirical expression for the Knox parameter C makes this comparison semi-quantitative.

In the preceding paper we have reported values of ρ^* for several proteins (both native and denatured) and shown that an equation similar to eqn. 21 accurately describes these ρ^* values:

$$\rho^* = 1 - 1.83\, r_{sp} + 1.21\, r_{sp}^3 - 0.38\, r_{sp}^5 \qquad (22)$$

Bandwidth data summarized in ref. 12 for the reversed-phase separation of peptides and proteins in the molecular-weight range $1300 \leqslant M \leqslant 80{,}000$ can be used to derive corresponding values of ρ^* in these systems. These data are summarized in Table I. As in ref. 12, use was made of runs with higher flow-rates (> 1 ml/min), where v' is larger and the term C of eqn. 1 plays a larger role. Derived values of ρ^* are therefore quite reliable. For similar reasons (larger values of v' desired), data for solutes with small M (and large D_m) were excluded in this initial comparison. Later in this paper we will report correlations between experimental bandwidth data and our model for all the solutes previously studied.

The ρ^* and r_{sp} values of Table I are plotted in Fig. 1, with eqn. 22 shown as the solid curve through these data. The fit of these data to eqn. 22 (the relationship

TABLE I

VALUES OF ρ^*, D_s/D_p AND r_{sp} DERIVED FROM BANDWIDTH DATA OF REFS. 12 AND 34. DENATURATION OF SOLUTE MOLECULES ASSUMED

See text and refs. 12 and 34 for details.

Solute	*M*	*Pore size (nm)*	ρ^*	r_{sp}	D_s/D_p
Leuc-enkephalin	600	14	*	0.10	0.20
Bradykinin	1100	14	*	0.12	**
Angiotensin I	1300	14	0.85	0.14	0.16
Glucagon	3500	14	0.80	0.23	0.20
Insulin	6000	14	0.75	0.30	0.24
Ribonuclease A	12 500	14	0.52	0.43	0.26
Lysozyme	14 000	14	0.31	0.46	0.14
Carbonic anhydrase	29 300	29	0.58	0.29	0.16
Transferrin	80 000	29	0.42	0.47	0.00

* Small M values (and small values of v') give inaccurate values of ρ^*.

** Bradykinin value of D_s/D_p is out of line (0.05), which is believed due to "non-well-behaved" nature of this solute.

previously derived from SEC data) is seen to be satisfactory, further confirming the basic soundness of our present model. The validity of eqn. 22 will therefore be assumed (as part of this model). However it should be stressed that predictions of ρ^* as in Fig. 1 (using eqn. 22) require that the conformation of the protein molecule be known (during its elution through the column).

Diffusion ratio D_s/D_p. Values of D_s/D_p for the reversed-phase separations of refs. 12 and 34 were derived from values of b' reported in ref. 12, using eqn. 12. These data are summarized in Table I and plotted *vs.* solute molecular weight M in Fig. 2. Also included in Fig. 2 is an average value of D_s/D_p from the extensive studies of small molecules ($300 \leqslant M \leqslant 400$) reported in ref. 5; this latter data-point (solid square in Fig. 2) is more reliable, since it represents a direct measurement of b' from values of B (eqn. 1).

The resulting data of Fig. 2 scatter considerably, reflecting difficulty in extracting accurate values of D_s/D_p from published data[12,34]. Nevertheless there is a clear

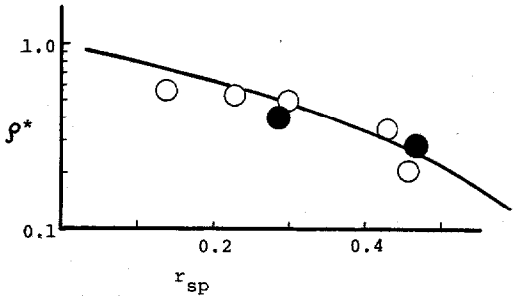

Fig. 1. Correlation of restricted-diffusion parameter ρ^* with r_{sp} = (solute Stokes diameter)/(pore diameter). Data of Table I for reversed-phase HPLC. ○, Data of ref. 12; ●, data of ref. 34.

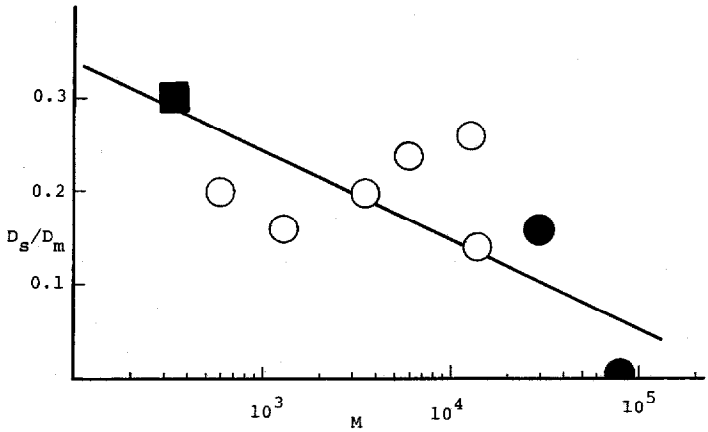

Fig. 2. Correlation of D_s/D_p with solute molecular weight. Data of Table I for reversed-phase HPLC. ○, Data of ref. 12; ●, data of ref. 34; ■, small-molecule data from ref. 5.

trend toward lower values of D_s/D_p for larger molecules, and this is reasonable. Large solute molecules with multiple attachments to the stationary phase surface would not be expected to undergo diffusion as easily as molecules in the mobile phase. Values of D_s/D_p for peptides and proteins can be predicted from the solid curve of Fig. 2:

$$\text{(reversed-phase)} \quad D_s/D_p = 0.52 - 0.094 \log M \tag{23}$$

over the range $500 \leqslant M \leqslant 100000$.

Plots of D_s/D_p *vs.* M for ion-exchange separation are also scattered (fewer data points); D_s/D_p values are generally about 1/3 as large as corresponding values (same value of M) for reversed-phase LC. This could have been anticipated, as strong interaction between solute molecules and sorption sites will decrease stationary phase diffusion*. Values of D_s/D_p can be predicted for ion-exchange HPLC (using previously measured b' values[14] and data of Kato cited below):

$$\text{(ion-exchange)} \quad D_s/D_p = 0.17 - 0.03 \log M \tag{24}$$

Overall correlation of experimental data with the present model

With the extensive modification and expansion of our model for HPLC protein separations, it is appropriate to compare the predictions of this model with bandwidth data treated earlier, using the original model. That is, how accurate is our model as a predictor of bandwidths? The original model employed several artificial fitting parameters (a', b', A and ρ) to achieve agreement with experimental data. The current model does not use arbitrary fitting parameters, with the exception of the column parameter A of eqn. 1 (see below). Therefore we might expect somewhat poorer correlative ability for our current model (fewer degrees of freedom). However our revised model should be more accurate in predicting bandwidths in the absence of experimental data. It is therefore of more general value.

* This is observed, for example, in separations on silica (adsorption chromatography *vs.* separation by reversed-phase LC; D_s/D_p is only 1/10 as great for silica (*cf.* b' values in ref. 5).

In addition to the numerous bandwidth data used to validate the original model, additional experimental studies from the literature have been tested *vs.* our revised model. Our choice of these literature studies is based on several considerations:

(1) A data base that covers a wide range of separation conditions, allowing a more critical test of the model's predictive ability.

(2) An absence of "non-ideal" effects as exhibited by tailing or misshapen elution bands, bands of widely varying width, etc.

(3) An adequate description of the separation system, including values for all experimental conditions.

The following data-base includes all studies which we are aware of that meet the above requirements and fall within the scope of our present model.

The Knox-parameter A. A varies with how well the column is packed, and should be measured for each column used with our model. However this was not done in the following correlations, with one exception (data of ref. 12). For the separation of large molecules under typical conditions, the effect of A on predicted values of bandwidth is usually small. For example, the ion-exchange study of Stout *et al.*[14] discussed below involved the proteins ribonuclease A and lysozyme ($12\,500 \leqslant M \leqslant 14\,000$). A change from 0.6 to 1.0 in the value of A assumed (a rather large change) resulted in an average increase in predicted bandwidth values of only 11%.

We have found that values of A for reversed-phase separations typically equal about 0.5, and this value was assumed with one exception (study of Meek and Rosetti[35], where data for a peptide sample are much better fit by $A = 1.4$). Likewise separations by IEC and SEC were best fit with A values of 1.0, which again were assumed for all such separations. These are probably not optimum values of A (with respect to these correlations); however the following correlations would not be improved much by further adjustment of this fitting-parameter. We have also observed that larger-pore packings generally give somewhat larger values of A *vs.* the case of packings with pores smaller than 20 nm.

Reversed-phase separations

Studies of Stadalius et al.[12]. Here seven peptides and proteins were run by gradient elution, varying conditions as follows: gradient time, 10–60 min; flow-rate, 1–4 ml/min; gradient range ($\Delta\varphi$), 0.25–0.40. The column used was 8 × 0.46 cm, with a 4.8-μm, 15-nm pore C_8 packing. The correlation between experimental and predicted bandwidth values is summarized in Table II. For 53 bandwidth values, the average value of R_w [equal to (experimental bandwidth/predicted bandwidth)] was $\bar{R}_w = 1.16$ [standard deviation] (S.D.) = 0.26)*, which means that experimental bandwidths were on average 16% higher than predicted.

The correlations for bradykinin ($\bar{R}_w = 1.30$) and lysozyme ($\bar{R}_w = 1.30$) suggest the possibility of non-ideal separations for these two compounds. If these data are omitted from the overall average, $\bar{R}_w = 1.10$ (S.D. = 0.21).

Studies of Cooke et al.[34]. Here five proteins** were run by gradient elution,

* Note that values of S.D. are with respect to $R_w = 1.00$ (not the mean of R_w values). The actual scatter of R_w values around mean values is generally much smaller than the value of S.D. cited.

** Data for two other proteins, bovine serum albumin (BSA) and ovalbumin, were not included. The bands for these two compounds are obviously distorted and wider than the bands for the remaining five proteins. We assume that BSA and ovalbumin are not "well-behaved" in this system.

TABLE II

SUMMARY OF EXPERIMENTAL *vs.* PREDICTED BANDWIDTHS FOR REVERSED-PHASE SEPARATIONS OF REFS. 12, 34 AND 35

$\bar{R}_w$ refers to average of experimental bandwidth divided by calculated bandwidth; S.D. is the standard deviation of R_w values *vs.* a value of $R_w = 1.00$; $A = 0.6$ for correlations of refs. 12 and 34; $A = 1.4$ for correlation of ref. 35.

Compound	*Ref.*	*n*	$\bar{R}_w$	*S.D.*	*M*
Leuc-enkephalin	12	8	1.03	0.24	600
Bradykinin	12	7	1.30	0.46	1100
Angiotensin I	12	8	1.20	0.30	1300
Glucagon	12	8	1.08	0.11	3500
Insulin	12	8	1.18	0.25	6000
Ribonuclease A	12	7	1.03	0.09	12500
Lysozyme	12	7	1.30	0.33	14000
Cytochrome *c**	34	15	0.81	0.22	12800
Carbonic anhydrase	34	13	1.09	0.16	29300
Transferrin	34	15	1.13	0.26	80000
Peptide mixture	35	17	1.04	0.10	1100

* Average values for three proteins of similar molecular weight (ribonuclease A, lysozyme), see ref. 12.

varying conditions as follows: gradient time, 6–392 min; flow-rate, 0.25–2 ml/min. The column used was 7.5 × 0.46 cm, with a 10-μm, 30-nm pore C_4 packing; $\Delta\varphi = 0.48$. The correlation between experimental and predicted bandwidths is summarized in Table II. For 43 bandwidth values, the average value of R_w was 1.01 (S.D. = 0.20), indicating close agreement (on average) between experimental and predicted bandwidth values.

Studies of Meek and Rosetti[35]. Here a mixture of peptides was run by gradient elution; average bandwidths for the mixture were reported. Conditions were varied as follows: gradient time, 8–80 min; flow-rate, 0.5–2.5 ml/min. The column used was 25 × 0.4 cm I.D. with a 10-μm, 8-nm pore packing. The correlation between experimental and predicted bandwidths is summarized in Table II. For 17 bandwidth values, values of $\bar{R}_w$ varied with A as follows: for $A = 1.0$, $\bar{R}_w = 1.16$ (S.D. = 0.17); for $A = 1.4$, $\bar{R}_w = 1.04$ (S.D. = 0.10). Agreement is significantly better if a somewhat poorly-packed column is assumed ($A = 1.4$). The column in question had been used

TABLE III

SUMMARY OF REVERSED-PHASE SEPARATIONS OF LYSOZYME DIGEST[12,13,17]. COMPARISON OF EXPERIMENTAL *vs.* PREDICTED VALUES

A equals 0.5 in all cases; other conditions given in refs. 12, 13, 17.

Ref.	*n*	$\bar{R}_w$	*S.D.*
12, 13	10	1.05	0.10
17	9	0.83	0.20

previously for other separations, so some degradation in its efficiency appears reasonable.

Lysozyme-digest separations of[12,13,17]. Here the same lysozyme digest was separated by reversed-phase gradient elution using different mobile phases (trifluoroacetic acid *vs.* phosphate buffer in acetonitrile–buffer gradients). Average bandwidths were determined and are compared with predicted values in Table III. For 19 different runs, $\bar{R}_w = 0.94$, (S.D. = 0.15), suggesting good agreement between experimental and predicted values for this "real" sample.

Ion-exchange separations

Studies of Stout et al.[14]. Here two proteins were run by ion-exchange HPLC, in both gradient and isocratic modes. Conditions were varied as follows: (gradient elution) gradient time, 10–80 min; flow-rate, 0.5–1 ml/min; (isocratic elution) k', 0.9–7. The column used was 8 × 0.62 cm, with a 7.5-μm, 30-nm pore packing of both weak and strong cation exchangers. The correlation between experimental and predicted bandwidths is summarized in Table IV. For 19 bandwidth values, $\bar{R}_w = 1.00$ (S.D. = 0.15); *i.e.*, close agreement between experimental and predicted values.

Studies of Kato et al.[36]. We have not previously analyzed these data. The protein ovalbumin was separated by gradient elution, with conditions varied as follows: gradient time, 30–360 min; flow-rate, 0.25–2 ml/min; column length, 7.5–15 cm. The column used was a nominal 25-nm pore packing, 10 μm in diameter. However for reasons discussed in a section below, we believe that the true pore-diameter for this column is 14 nm (ref. 15). Table V gives experimental and predicted bandwidth values for individual runs reported by these workers. Overall agreement for these 19 bandwidth values is good: $\bar{R}_w = 1.07$ (S.D. = 0.11).

The similar prediction of retention data from this study is described in ref. 4. That correlation also yielded a value of $m = 8.8$ for this system (required in predictions by our model).

Size-exclusion separations

Study of Ghrist et al.[15]. Comparison of experimental and predicted bandwidth values is provided in the preceding paper. Twelve proteins were run on two different SEC columns, using mobile phases that either retained the native protein conformation or caused denaturation. Two protein/column systems were found to be "non-ideal". Excluding the latter runs, 55 bandwidth values gave $\bar{R}_w = 1.04$ (S.D. = 0.07). This represents excellent agreement between experimental data and the model.

TABLE IV

SUMMARY OF EXPERIMENTAL *vs.* PREDICTED BANDWIDTHS FOR THE ION-EXCHANGE SEPARATIONS OF STOUT *et al.*[14]

A equals 1.0; other conditions given in ref. 14.

Compound	*Elution mode*	*n*	$\bar{R}_w$	*S.D.*	*M*
Ribonuclease A	Gradient	7	0.88	0.32	12 500
Lysozyme	Gradient	7	1.07	0.16	14 000
	Isocratic	5	1.05	0.09	14 000

TABLE V

EXPERIMENTAL *vs.* PREDICTED BANDWIDTHS FOR ION-EXCHANGE SEPARATIONS OF OVALBUMIN BY KATO *et al.*[36]

Column length (cm)	*Gradient time t_G (min)*	*Flow-rate (ml/min)*	*t_g (min)*	*Bandwidths (s)*	
				Expt.	*Calc.**
15	30	1.0	13.2	14	15
	45		16.4	18	17
	60		19.1	21	21
	90		23.7	28	25
	120	1.0	27.8	31	27
	180		34.4	43	37
	240		39.9	52	45
	360		49.6	71	58
	30	2.0	9.4	14	13
	120	0.5	37.5	33	32
	240	0.25	75	60	50
7.5	30	1.0	9.7	14	14
	45		12.1	17	17
	60		14.3	21	21
	90		18.0	28	26
	120		21.0	33	32
	180		26.1	44	41
	240		30.4	53	50
	360		37.6	74	65

* Conditions assumed: column diameter, 0.6 cm; particle size, 10 μm; $A = 1.0$; $x = 0.44$; $M = 44000$, $T = 25$°C; mobile phase viscosity at 25°C = 0.95; $m = 8.8$; salt gradient from 0.1 to 0.3 M.

TABLE VI

COMPARISON OF EXPERIMENTAL AND CALCULATED BANDWIDTHS FOR HIC (STUDY OF REF. 37) AVERAGE BANDWIDTHS FOR RIBONUCLEASE A AND CHYMOTRYPSINOGEN

Conditions: 10 × 0.46 cm column of 6-μm 29-nm pore particles, 25°C, flow-rate = 1.0 ml/min; $A = 1.0$; viscosity at 25°C = 1.45 cPoise, $x = 0.6$; $\lambda = 2$; $c_0 = 4\ M$; $c_f = 0.5\ M$; calc. 1 assumes native proteins; calc. 2 assumes denatured proteins.

Gradient time (min)	*Bandwidths σ (s)*		
	Expt.	*Calc. 1*	*Calc. 2*
2	3.7	2.0	2.8
3	2.8	2.2	3.2
5	3.2	2.7	4.0
10	5.9	3.7	5.8
15	7.8	4.0	7.0
18	8.5	4.4	7.7
20	9.6	5.0	8.2
36	13.8	6.6	11.3
45	14.1	7.4	12.9
60	17.3	8.7	15.4
$\bar{R}_w$		1.73	1.08
S.D.		0.79	0.14

Hydrophobic-interaction chromatography separations

Study of Miller and Karger[37]. Here ribonuclease A and chymotrypsinogen were run by gradient elution, and bandwidths for the two proteins were averaged for each gradient condition. Gradient times were varied from 2 to 60 min; the column was 10 × 0.46 cm, with 6-μm particles and 30-nm pores. The comparison of experimental and predicted bandwidths is shown in Table VI. The initial application of our model assumed the native molecule, but the resulting correlation (calc. 1 in Table VI) is poor: $\bar{R}_w = 1.73$ and S.D. = 0.79. That is, experimental bandwidths are 73% greater (on average) *vs.* predicted values.

An explanation for this observation is suggested by recent work of Wu *et al.*[38]. They studied the *in situ* denaturation of several proteins during HIC separation and found that reversible denaturation occurred. At low temperatures the native protein is favored, while at higher temperatures the denatured protein predominates. As a result, bandwidths at intermediate temperatures were generally larger, due to co-elution of native and denatured species. Thus in the case of the proteins of Table VI (ribonuclease A and chymotrypsinogen), the observed bandwidths could be wider than predicted for either of two reasons: separation of each protein as the totally denatured species, or as a mixture of native plus denatured conformations. We checked the former possibility (denatured proteins during separation) by assuming totally denatured compounds during elution, with a corresponding change in values of D_m and d_s. The resulting calculations (calc. 2 in Table VI) are seen to correlate better with the experimental data: $\bar{R}_w = 1.08$, S.D. = 0.14. We do not know at this point whether the separations of Karger and co-workers[37,38] actually involve the denatured molecule. The data of Table VI suggest that this is the case, but further work will be required to document protein conformation during HIC separation for this system (see further discussion in ref. 30). At the moment, final conclusions are not possible.

Pore size determinations. These have been discussed by Warren and Bidlingmeyer[39] and Knox and Scott[40], for column packings of the type under discussion. The preferred approach seems to be measurement of pore size under chromatographic conditions, using a sample–mobile phase combination that yields $k' = 0$ (no retention by the stationary phase). Most packings are described in terms of the pore diameter of the silica particles used prior to bonding. However the usual mono-layer bonded silica packings will have their pore diameters reduced by about 1 nm on average, and we have used this figure in adjusting the nominal pore diameters of the columns reviewed in this paper. Exceptions are the TSK ion-exchange columns of Table V. These packings derive from a TSK G3000SW packing (diol-silica SEC column), whose retention characteristics are similar to that of the GF-250 column referred to in ref. 15. Therefore[39,40] it can be surmised that the pore diameters of these two columns are similar. For this reason we have taken the pore diameter of the columns of Table VI equal to 14 nm, rather than the nominal 25-nm value for the starting silica. The smaller pore size for these TSK packings probably reflects the use of a polymerized (thick) layer of the diol bonded phase.

DISCUSSION AND CONCLUSIONS

The present model is an attempt at both a comprehensive and detailed descrip-

tion of the HPLC separation of peptide and protein samples. We believe that all of the physico-chemical effects involved in these separations have now been taken into account. While the model is based on the same basic principles that apply to chromatography in general, the various special characteristics of protein molecules are recognized. Specifically we have seen that protein conformation can have a major effect on bandwidth. This arises directly from the dependence of values of D_m and ρ^* on conformation, and indirectly from changes in conformation during separation (*e.g.* refs. 41–45).

We further believe that when experimental bandwidths are significantly larger than values predicted by our model (*e.g.* 50% or more), this reflects a "non-well-behaved" system. Examples of such effects have been presented in the preceding paper for SEC[15]. Changes in protein conformation during separation are one such effect that can cause excess band broadening. Other possible non-ideal effects are discussed in refs. 15 and 30. The better understanding and practical elimination of these non-ideal effects probably represent the single largest opportunity for any major improvement in the HPLC separation of proteins larger than 30 000 Dalton.

If we consider only "well-behaved" systems in the correlations summarized in the preceding section, we find that the model predicts experimental bandwidths with an overall accuracy of ± 17% (1 S.D.). Considering the complexity of these systems, and the practical insignificance of errors of this magnitude, we feel that our model has performed as well as we could expect. We further note that the experimental measurement of protein bandwidths is frought with numerous problems, and the scatter in such measurements is often about ± 5–10%.

The present model can be used in a number of different ways, to answer questions of both practical and fundamental interest. We have seen how general calculations from the model can be used to optimize the separation potential of different HPLC methods for separating peptides and proteins (e.g., Fig. 3 of ref. 15 and review of ref. 30). We have also shown how similar calculations can be used to guide the development of HPLC methods for specific samples (reversed-phase separation of peptides[13] and ion-exchange separation of ovalbumin[14]. The model has also been used to evaluate the relative merits of different columns for peptide separations[17], and to discuss the features required in optimum columns for specific applications[30]. We hope in future reports to show that the model can shed new light on "non-well-behaved" systems, and lead the way to improved separations in these cases.

Changes in conditions that avoid excess band-broadening will generally favor maximum mass-recovery of the sample. The preceding discussion can serve as a guide, but much remains to be learned. There seems to be a trend toward lower protein recovery for longer gradient times, in both reversed-phase[46] and ion-exchange[47] separation. Since longer gradient times favor maximum sample resolution, this means that there may sometimes be a conflict between maximum resolution and maximum recovery. In some cases this can be resolved by using a reduced gradient range (smaller change in φ or c during the gradient), which for some samples is an alternative to increasing gradient time. For example, this is always applicable when only one compound in the sample is to be recovered in purified form.

A more basic question concerns the physical processes involved in the HPLC separation of macromolecules. We have assumed in our model that these processes are essentially the same as determine the similar separation of small molecules. How-

ever this is still an area of considerable controversy. Other workers have proposed that the basis of these large-molecule separations differs in fundamental respects from corresponding HPLC separations of compounds with $M > 10000$ (see reviews of refs. 9 and 30). In this respect the ability of the present model to accurately describe bandwidths (review of present paper) and retention (see refs. 4, 11, 14, 30 and 37 and cited refs.) represents strong evidence to the contrary.

Further substantiation of a "normal-chromatographic" basis for separations of proteins by HPLC is provided by a recent report of Di Bussolo and Gant[48]. These workers reported the direct observation of protein migration during reversed-phase HPLC (using glass columns and colored proteins); their results are consistent with predictions from the present model, and rule out a number of other possibilities that have been proposed.

APPENDIX I

Examples of calculations by the model

The examples shown in Table AI illustrate the application of the model for reversed-phase and ion-exchange gradient elution, and isocratic separation by SEC. The examples correspond to actual experimental runs reported here or earlier.

APPENDIX II

Further discussion of dependence of D_m on pressure

In our original study of bandwidths for small molecules[5], larger flow-rates and column pressures were encountered. Re-examination of these data indeed shows that values of C for 3-μm columns tend to be larger than for 6-μm columns, other conditions similar. Since the 3-μm particle studies generally involved higher column pressures (with corresponding smaller values of v) an increase in D_m with pressure would qualitatively account for this discrepancy. The consequences of this pressure effect in the study of ref. 5 were minimized, however, by certain other factors. Thus the data system used in ref. 5 did not allow reliable measurement of bands that were quite narrow. These data points could be recognized by certain characteristics of the band, and were discarded before values of A, B and C were extracted from a given set of data. Since narrow bands are generally associated with small-particle columns and high flow-rates, those data most susceptible to pressure effects were discarded for other reasons. The data of ref. 5 were further manipulated to yield similar ("predetermined") values of A for different columns of the same type (*e.g.*, C_8 or C_{18} columns, 3- or 6-μm particles), since it was believed that these various columns (packed from similar materials in the same way) should yield roughly constant values of A. The analysis of C values in ref. 5 was based mainly on these smoothed values of A.

As a result of these fortuitous circumstances, the actual impact of pressure-dependent D_m values on the final conclusions of ref. 5 appears to have been minimal. Other workers[49,50] have noted that high pressures generally coincide with higher flow-rates, with a resulting increase in column temperature (beyond that of the constant-temperature bath). It was then argued[49] that the higher column temperature increases D_m, which serves to effectively cancel the lowering of D_m values by higher

TABLE AI

EXAMPLES OF CALCULATIONS BY THE MODEL

Input data (separation conditions) are listed first, followed by serial calculations as required in the model.

Parameter	*Equation**	*Values***		
		RPC	*IEC*	*SEC*
Column				
length, L (cm)	Input data	8	8	25
diameter, d_c (cm)	Input data	0.62	0.62	0.94
particle size, d_p (cm)	Input data	0.00048	0.00075	0.0004
d_{pore} (nm)	Input data	14	29	14
x value	Input data	0.67	0.6	0.63
A value	Input data	0.5	1.0	1.0
Temperature, T (°C)	Input data	35	25	25
Viscosity, n_{25} (cPoise)	Input data	0.95	1.0	1.0
Solute mol. wt., M (M_d)	Input data	12 500	12 500	162 000
Gradient range				
RP, $\Delta\varphi$	Input data	0.30		
IEC, c_0	Input data		0.02	
c_f	Input data		1.02	
Gradient time, t_G (min)	Input data	40	40	
Retention parameters	Input data			
RP, S	Input data	***		
IEC, t_g (min)	Input data		10.8	
m	Input data		3.8	
V_D (ml)	Input data		1.4	
SEC, K_D	Input data			0.33
Flow-rate, F (ml/min)	Input data	2.0	1.0	4.5
Column volume, V_m (ml)	II-6	1.44	1.61	11.0
Dead-time, t_0 (min)	V_m/F	0.72	1.61	2.44
Solute				
denatured mol. wt., M_d	I-15	83 000	–	–
diff. coef. D_m (cm^2/s)	I-16b	$7.2 \cdot 10^{-7}$	$1.01 \cdot 10^{-6}$	$4.2 \cdot 10^{-7}$
diff. coeff. D_{mw}	I-16c	$6.1 \cdot 10^{-7}$	$1.13 \cdot 10^{-6}$	$4.6 \cdot 10^{-7}$
Stokes diam. d_s (nm)	I-18	5.6	3.0	7.4
r_{sp}	d_s/d_{pore}	0.40	0.10	0.53
	I-19	0.34	0.80	0.20
D_s/D_p				
RP	II-23	0.133		
IEC	II-24		0.047	
S	$0.48\ M^{0.44}$ (ref. 11)	30.5		
$\bar{k}$ (refs. 11, 14)				
RP	§	5.3		
IEC	§§		2.38	
p	§§§		1.40	
B	II-10	1.31	1.30	0.90
C	II-13a, 14	0.079	0.051	0.036

TABLE AI (*continued*)

Parameter	*Equation**	*Values***		
		RPC	*IEC*	*SEC*
Mobile phase				
velocity, u' (ml/s)	II-4	0.276	0.138	0.27
red velocity, v'	II-5	183	102	260
Solute				
h	II-1	17.4	9.9	15.6
N	L/hd	960	1080	4000
Bandwidth calc. (ref. 12)†				
J	12†	1.24	1.45	
Peak width σ_v (ml)	11a†	0.181	0.120	0.131
Peak width σ_t (s)	14†	5.4	7.2	1.74
Peak capacity PC	16†	111	83	

* I-2 and II-3 refer, respectively, to eqn. 2 of ref. 15 (Part I) and eqn. 3 of the present paper (Part II).

** RPC, IEC and SEC refer, respectively to separation by reversed-phase, ion-exchange and size-exclusion chromatography.

*** An experimental value of S can be used, and this is preferable; alternatively S can be estimated as indicated above.

§ $t_G F/1.15\ V_m \Delta\varphi S$.

§§ $t_G F/1.15\ V_m[\log(c_F/c_0)]\ mr$.

§§§ r can be assumed equal to 1.00 for average calculations; r can also be estimated from Table I of ref. 14; finally, the most precise value (given here) is calculable as described in ref. 14.

† The equations cited here are from ref. 12.

pressures. At this time it appears that these pressure-related effects are probably of minor importance in determining the bandwidths of protein solutes in typical HPLC separations.

REFERENCES

1 L. R. Snyder, in Cs. Horváth (Editor), *High-Performance Liquid Chromatography. Advances and Perspectives*, Vol. 1, Academic Press, New York, 1980, p. 207.
2 M. A. Quarry, R. L. Grob and L. R. Snyder, *J. Chromatogr.*, 285 (1984) 1.
3 M. A. Quarry, R. L. Grob and L. R. Snyder, *J. Chromatogr.*, 285 (1984) 19.
4 M. A. Quarry, R. L. Grob and L. R. Snyder, *Anal. Chem.*, 58 (1986) 907.
5 R. W. Stout, J. J. DeStefano and L. R. Snyder, *J. Chromatogr.*, 282 (1983) 263.
6 L. R. Snyder and P. E. Antle, *LC Liq. Chromatogr. HPLC Mag.*, 3 (1985) 98.
7 J. P. Larmann, J. J. DeStefano, A. P. Goldberg, R. W. Stout, L. R. Snyder and M. A. Stadalius, *J. Chromatogr.*, 255 (1983) 163.
8 M. A. Quarry, M. A. Stadalius, T. H. Mourey and L. R. Snyder, *J. Chromatogr.*, 358 (1986) 1.
9 M. A. Stadalius, M. A. Quarry, T. H. Mourey and L. R. Snyder, *J. Chromatogr.*, 358 (1986) 17.
10 L. R. Snyder, M. A. Stadalius and M. A. Quarry, *Anal. Chem.*, 55 (1983) 1412A.
11 M. A. Stadalius, H. S. Gold and L. R. Snyder, *J. Chromatogr.*, 296 (1984) 31.
12 M. A. Stadalius, H. S. Gold and L. R. Snyder, *J. Chromatogr.*, 327 (1985) 27.
13 M. A. Stadalius, M. A. Quarry and L. R. Snyder, *J. Chromatogr.*, 327 (1985) 93.
14 R. W. Stout, S. I. Sivakoff, R. D. Ricker and L. R. Snyder, *J. Chromatogr.*, 353 (1986) 439.
15 B. F. D. Ghrist, M. A. Stadalius and L. R. Snyder, *J. Chromatogr.*, 387 (1987) 1.

16 J. L. Glajch, M. A. Quarry, J. F. Vasta and L. R. Snyder, *Anal. Chem.*, 58 (1986) 280.
17 A. J. Banes, G. W. Link and L. R. Snyder, *J. Chromatogr.*, 326 (1985) 419.
18 M. T. W. Hearn and B. Grego, *J. Chromatogr.*, 255 (1983) 125.
19 N. T. Miller, B. Feibush and B. L. Karger, *J. Chromatogr.*, 316 (1985) 519.
20 N. T. Miller and B. L. Karger, *J. Chromatogr.*, 326 (1985) 45.
21 M.-I. Aguilar, A. N. Hodder and M. T. W. Hearn, *J. Chromatogr.*, 327 (1985) 115.
22 M. T. W. Hearn and M. I. Aguilar, *J. Chromatogr.*, 352 (1986) 35.
23 M. T. W. Hearn and M. I. Aguilar, *J. Chromatogr.*, 359 (1986) 31.
24 J. H. Knox, *J. Chromatogr. Sci.*, 15 (1977) 352.
25 J. C. Giddings, *Dynamics of Chromatography*, Marcel Dekker, New York, 1965.
26 M. Martin and G. Guiochon, *Anal. Chem.*, 55 (1983) 2302.
27 M. Martin, personal communication.
28 W. R. Melander, D. Corradini and Cs. Horváth, *J. Chromatogr.*, 317 (1984) 67.
29 M. G. Kunitani, D. J. Johnson and L. R. Snyder, *J. Chromatogr.*, 371 (1986) 313.
30 L. R. Snyder and M. A. Stadalius, in Cs. Horváth (Editor), *Advances in High-performance Liquid Chromatography*, Vol. 4, Academic Press, New York, 1986, in press.
31 C. N. Satterfield, C. K. Colton and W. H. Pitcher, *AIChE J.*, 19 (1973) 628.
32 R. R. Walters, *J. Chromatogr.*, 242 (1982) 19.
33 M. T. W. Hearn and B. Grego, *J. Chromatogr.*, 282 (1983) 541.
34 N. H. C. Cooke, B. G. Archer, M. J. O'Hara, E. C. Nice and M. Capp, *J. Chromatogr.*, 255 (1983) 115.
35 J. L. Meek and Z. L. Rosetti, *J. Chromatogr.*, 211 (1981) 15.
36 Y. Kato, K. Komiya and T. Hishimoto, *J. Chromatogr.*, 246 (1982) 13.
37 N. T. Miller and B. L. Karger, *J. Chromatogr.*, 326 (1985) 45.
38 S.-L. Wu, K. Benedek and B. L. Karger, *J. Chromatogr.*, 359 (1986) 3.
39 F. V. Warren, Jr. and B. A. Bidlingmeyer, *Anal. Chem.*, 56 (1984) 950.
40 J. H. Knox and H. P. Scott, *J. Chromatogr.*, 316 (1984) 311.
41 S. A. Cohen, K. P. Benedek, S. Dong, Y. Tapui and B. L. Karger, *Anal. Chem.*, 56 (1984) 217.
42 K. Benedek, S. Dong and B. L. Karger, *J. Chromatogr.*, 317 (1984) 227.
43 S. A. Cohen, S. Dong, K. P. Benedek and B. L. Karger, in *Symposium Proceedings, 5th International Symposium on Affinity Chromatography and Biological Recognition*, Academic Press, New York, 1984, p. 479.
44 K. A. Cohen, K. Schnellenberg, K. Benedek, B. L. Karger, B. Grego and M. T. W. Hearn, *Anal. Biochem.*, 140 (1984) 223.
45 M. T. W. Hearn, A. N. Hodder and M.-I. Aguilar, *J. Chromatogr.*, 327 (1985) 47.
46 N. H. C. Cooke, B. G. Archer, M. J. O'Hare, E. C. Nice and M. Capp, *J. Chromatogr.*, 255 (1983) 115.
47 Y. Kato, K. Nakamura and T. Hashimoto, *J. High Resolut. Chromatogr. Chromatogr. Commun.*, 8 (1985) 154.
48 J. M. Di Bussolo and J. R. Gant, *J. Chromatogr.*, 327 (1985) 67.
49 E. Katz, K. Ogan and R. P. W. Scott, *J. Chromatogr.*, 260 (1983) 277.
50 E. D. Katz and R. P. W. Scott, *J. Chromatogr.*, 270 (1983) 29.